Journal of the Civil Engineering Forum, May 2026, 12(2):255-266
DOI 10.22146/jcef.22477
Available Online at https://jurnal.ugm.ac.id/v3/jcef/issue/archive

Unconfined Compressive Strength and Damage Evolution in Geopolymer-Stabilized Clay Shale: Role of Temperature and Alkali Activator Ratio

Willis Diana[1*], Edi Hartono[1], Agus Setyo Muntohar[1], Nurza Purwa Abiyoga[2]
[1]Department of Civil Engineering, Universitas Muhammadiyah Yogyakarta, Yogyakarta, INDONESIA
[2]Department of Civil Engineering, Universitas Jambi, Jambi, INDONESIA
*Corresponding author: willis.diana@umy.ac.id

SUBMITTED 20 June 2025 **REVISED** 05 October 2025 **ACCEPTED** 06 October 2025

ABSTRACT Exposed clay shale is highly susceptible to weathering and rapid strength degradation, which often leads to slope and earth-structure instability. Geopolymer-based soil stabilization has emerged as a promising method to improve the mechanical properties of such problematic materials. However, this chemical stabilization process is sensitive to environmental conditions, particularly temperature fluctuations. The performance of geopolymer-stabilized clay shale under elevated-temperature conditions remains insufficiently investigated, particularly in tropical regions such as Indonesia, where temperatures can fluctuate between 25°C and 40°C, and the exposed ground surface may reach up to 60°C during the dry season because of intense solar radiation. This study evaluates the effectiveness of fly ash–based geopolymer in stabilizing clay shale under temperature variations ranging from 26°C to 60°C. A series of laboratory experiments was conducted using two alkali activator ratios (Na_2SiO_3:NaOH), namely 2.0 (Ratio A) and 2.5 (Ratio B). Mechanical performance was assessed through unconfined compressive strength (UCS) tests, stress–strain analysis, and energy-based damage evolution to quantify strength development and failure behavior. The results indicate that temperature is the dominant factor controlling strength development. A 10°C increase in curing temperature resulted in a 40–60% increase in UCS, whereas variations in the alkali activator ratio produced only a 15–20% increase. The highest strength amplification, reaching 16 times that of untreated soil, was achieved using Ratio B at 60°C, while Ratio A showed strength stagnation above 50°C. Microstructural observations suggest that elevated temperatures accelerate geopolymer gel formation, leading to higher initial stiffness and an expanded elastic region. However, this also resulted in more brittle behavior, characterized by a higher brittleness index and rapid post-peak damage propagation for Ratio B, whereas Ratio A exhibited greater ductility. Overall, higher curing temperatures increased the dissipated energy at failure and revealed a clear strength–ductility trade-off. These findings provide insights for optimizing geopolymer stabilization of clay shale, particularly for geotechnical applications in tropical environments where elevated in situ temperatures are common.

KEYWORDS Alkali Activator Ratio; Clay Shale; Damage Properties; Geopolymer Stabilization; Temperature.

1 INTRODUCTION

Chemical stabilization is commonly employed to improve the geotechnical properties and engineering performance of problematic soils, particularly through the use of cement–based binders. However, cement manufacturing has significant environmental impacts. For instance, producing one ton of cement generates approximately 0.95 tons of CO_2 emissions and requires about 5000 MJ of energy (Miraki et al., 2022). In addition to environmental concerns, cement-stabilized soils often exhibit substantial plastic shrinkage. Water loss and inadequate curing conditions may also lead to incomplete hydration during the early stages, resulting in reduced strength development. This issue becomes more pronounced in regions with high annual temperatures, where extensive wet curing over large construction sites is often impractical (Ghadir and Ranjbar, 2018). Consequently, considerable attention has been directed toward developing alternative binders with lower environmental impacts.

Several alternative materials have been investigated for soil chemical stabilization, including lime, fly ash, rice husk ash, kiln dust, and other recycled materials or by–products with high alumina (Al_2O_3) and silica (SiO_2) (Ayub and Khan, 2023). The development of these aluminosilicate–rich materials has led to the emergence of geopolymer binders as a sustainable alternative to conventional cement. Geopolymers are synthesized through polymerization reaction between precursors with high silica and alumina content and alkali activators (Xu and Van Deventer, 2002). The geopolymerization process begins with the dissolution of amorphous aluminosilicate materials (precursor) in alkaline hydroxide and/or alkaline silicate solutions, producing reactive silica and alumina. The dissolved precursor's silica and alumina subsequently un-

dergo polycondensation, forming amorphous or semi–crystalline oligomers that further polymerize and solidify into synthetic aluminosilicate materials (Zhang et al., 2013). When the precursor contains low calcium content, the resulting geopolymer structure is dominated by Si–O–Al–O bonds forming three-dimensional polymeric chains and ring structures, rather than calcium silicate hydrate (C–S–H) gels typically observed in cement hydration reactions (Wong et al., 2019).

In geopolymerization, the alkali activator provides the necessary alkalinity to dissolve aluminosilicate materials in the precursor and acts as a catalyst that speeds up the polymerization reaction. The type and concentration of alkali activator strongly influence the reaction rate and the final properties of the geopolymer. Common alkali activators for geopolymer include sodium silicate (Na_2SiO_3) or potassium silicate (K_2SiO_3), often combined with sodium hydroxide (NaOH) or potassium hydroxide (KOH) (Abdullah and Ahmad, 2017). Although geopolymerization can occur using a single alkaline activator, higher reaction rates are generally achieved when alkaline hydroxide solutions are combined with soluble silicate solutions. Mixtures of sodium silicate and sodium hydroxide have been shown to enhance stabilization performance (Abdullah et al., 2015; Van Deventer et al., 2007). Nevertheless, determining the appropriate alkali activator ratio, particularly the ratio of sodium silicate to sodium hydroxide, remains challenging, given the distinct characteristics of different soil types.

Geopolymer-based soil stabilization has demonstrated promising performance in a wide range of soils. Previous studies have reported successful geopolymer application in sandy soils (Diana, Hartono and Kusuma, 2025; Diana, Ma'rifah and Hartono, 2025; Razeghi et al., 2024), expansive fine-grained soils (Diana, Hartono and Damayanti, 2025; Khasib et al., 2021), and highly acidic soft soils such as peat (Khanday et al., 2021; Luo and Zhang, 2023). Despite these advances, the application of geopolymer stabilization to easily degradable materials such as clay shale remains limited. Clay shale, classified as a type of mud rock, can experience a drastic reduction in shear strength when exposed to atmospheric conditions and water (Hartono et al., 2021). Understanding the stabilization behavior of clay shale is therefore important for improving the durability and engineering performance of this material (Simatupang et al., 2022).

In practical field applications, stabilized soils are exposed to environmental temperatures that may influence geopolymerization and long-term strength development. Moreover, increasing environmental temperatures associated with climate change may further affect the performance of chemically stabilized soils. Indonesia experiences a tropical climate with temperatures typically ranging from 25°C to 40°C, and annual rainfall of 2700–2900 mm/year. These climatic conditions can accelerate clay shale degradation in the field, thereby contributing to slope instability. Improving the stability of clay shale slopes is therefore an important geotechnical challenge in many regions of Indonesia. At the same time, the country produces large quantities of fly ash as an industrial by-product, which can potentially be utilized as a precursor material for geopolymer stabilization. These conditions provide a strong motivation to explore geopolymer–based stabilization for clay shale. Therefore, this study investigates the effect of temperature on the strength characteristics of geopolymer–stabilized clay shale. The unconfined compressive strength behavior of stabilized specimens is evaluated under varying curing temperatures and activator mixture ratios. In addition, stress–strain behavior and energy dissipation analysis are used to examine damage evolution mechanisms during loading. This study clarifies the influence of temperature on strength development and failure characteristics of geopolymer–stabilized clay shale and identifies the optimum activator ratio for practical applications.

2 METHODS

Unconfined compressive strength (UCS) test was conducted to determine the compressive strength of the treated soil specimens under unconfined conditions. Eight sample groups (Table 1) comprising three specimens were prepared to evaluate the effect of curing temperature and alkali activator ratio. All specimens were treated with the same activator molarity (i.e., 12M) and curing time (i.e., 7 days). A 12M NaOH solution was selected as the activator, aligning with prior geopolymer-clay studies (e.g., Provis, 2009) and preliminary tests result, which indicated optimal strength-to-durability performance (Hartono, Diana and Hendriana, 2023). A curing period of seven days is considered sufficient for preliminary evaluation and initial strength assessment (Rivera et al., 2020). The alkali activator ratio (Na_2SiO_3:NaOH) was set at 2.0 (Ratio A) and 2.5 (Ratio B). The curing temperatures varied to 26°C, 40°C, 50°C, and 60°C, with 26°C representing room temperature. The specimen cured at room temperature was used as the control to evaluate the effect of curing temperature. Table 1 presents detailed information for the experimental design. The first letter in the sample code represents the alkali activator ratio, while the following two numbers indicate the curing temperature.

2.1 Clay Shale

The soil sample was collected from the cut slope along the Bawen-Semarang toll road. Figure 1 shows the clay shale boulder collected from the study site. The spe-

Table 1. Details of samples treatment

Sample Group	Number of Specimen	Activator Ratio (Na_2SiO_3: NaOH)	Curing Temperature (°C)
A26	3	2.0:1	26
A40	3	2.0:1	40
A50	3	2.0:1	50
A60	3	2.0:1	60
B26	3	2.5:1	26
B40	3	2.5:1	40
B50	3	2.5:1	50
B60	3	2.5:1	60

cific gravity of the soil was 2.65. The clay shale comprised 7% sand and 93% clay. The liquid limit, plastic limit, and plasticity index were 58%, 28%, and 29%, respectively. The sample was classified as a high plasticity clay (CH) according to the Unified Soil Classification System. X–ray diffraction analysis indicated that the clay shale mineral composition was dominated by smectite/montmorillonite (34%), with smaller fractions of illite, kaolinite, chlorite, calcite (24%), and quartz (33%). The maximum dry density and the optimum moisture content (OMC) from the Standard Proctor test were 16.3 kN/m^3 and 19%, respectively.

Figure 1. Clay shale from Bawen-Semarang Toll Road.

2.2 Geopolymer

Class F fly ash was used as the precursor for geopolymer synthesis, which contains up to 70% silica, alumina, and ferric, with less than 10% calcium. Fly ash was collected from coal–fired power plants and is readily available as an industrial by–product that often creates waste management challenges. Sodium silicate (Na_2SiO_3) and sodium hydroxide (NaOH) were used as alkali activators to promote the geopolymerization reaction. The sodium hydroxide used in this study was in a solid flake form, which was later dissolved with liquid sodium silicate. The solution mixture was diluted with water to reach a molarity of 12M, as previous studies have shown that Na_2SiO_3+NaOH mixtures with molarities of 12–14 M provide superior stabilization performance (Abdullah et al., 2011; Hartono, Diana and Bahti, 2023).

2.3 Specimen Preparation and Testing

The clay shale boulder was crushed into small fragments and sieved using a 4.75 mm sieve. The dry soil was mixed with 15% fly ash by total weight and stirred in the stirring machine. The 15% fly ash content was selected based on literature recommendations for the stabilization of high-plastic clay soils, where fly ash contents between 10% and 20% are considered most effective (Abdullah et al., 2015; Phetchuay et al., 2016; Zhang et al., 2013). The activator was then poured gradually into the mixture and stirred until a homogenous slurry was formed. The amount of activator added was 19% of the total mixture weight. The activator dosage (19% by weight) matched the untreated soil's OMC to ensure sufficient moisture for geopolymerization while maintaining workability. The mixtures were placed into the cylindrical mold with a height of 76 mm and an inner diameter of 38 mm, followed by compaction through static pressing to achieve the target dry density of 16.3 kN/m^3.

The specimens were cured for seven days prior to testing under two different curing regimes. The first group was cured at room temperature (26°C), under natural laboratory humidity of 70–85% relative humidity (RH) and served as the control condition. The second group was cured in a temperature-controlled oven at 40°C, 50°C, and 60°C, where the RH was approximately 30% due to moisture reduction at elevated temperatures. These temperatures were selected to evaluate the effect of moderate thermal curing on geopolymerization and strength development, since the range of 40–60°C

is widely used to accelerate aluminosilicate dissolution and early binder formation while avoiding severe drying damage. The maximum temperature was limited to 60°C to reduce the risk of excessive moisture loss, shrinkage cracking, and strength deterioration. Air circulation fans were used to maintain a uniform temperature within the oven chamber. Although humidity was not actively controlled, both curing environments were considered representative of practical field conditions.

The UCS test was conducted in accordance with ASTM D2166. The specimen was axially loaded at a rate of 0.76 mm/min until it reached the maximum load and failed. The load and deformation were measured using a load cell and digital dial gauge, respectively, and were continuously recorded by data logger to construct the stress and strain curve (Figure 2). The unconfined compressive strength (q_u) was calculated by dividing the maximum axial load (F_{max}) by the area (A) as written in Equation 1. The stress-strain properties, such as brittleness index (I_B) and secant modulus (E_{50}), were calculated from the stress-strain curve. The brittleness index was obtained by dividing the deviation of the maximum stress (q_u) and the residual stress (q_r) by the maximum stress (q_u) (Equation 2). The I_B ranges from 0 (ductile) to 1 (brittle). The secant modulus was defined as the slope of the stress-strain curve between the initial point and the stress-strain at 50% of the maximum stress (q_{u50}) along with its corresponding strain (ε_{u50}) (Equation 3).

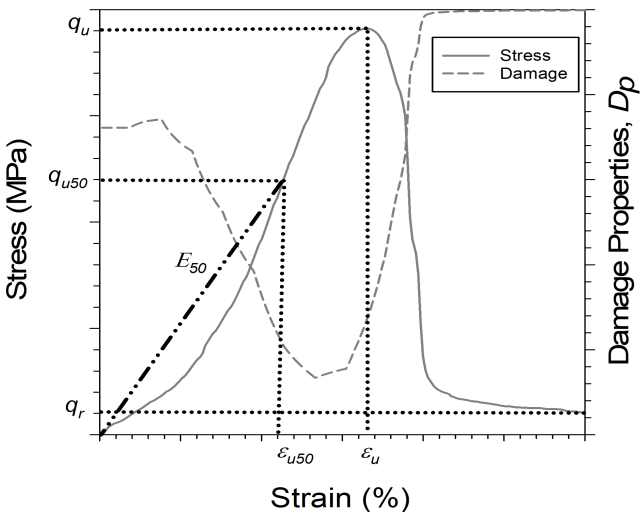

Figure 2. A typical stress–strain curve and its properties determination.

$$q_u = \frac{F_{\max}}{A} \tag{1}$$

$$I_B = \frac{q_u - q_r}{q_u} \tag{2}$$

$$E_{50} = \frac{q_{u50}}{\varepsilon_{u50}} \tag{3}$$

Damage and failure mechanisms during loading were analyzed using an energy dissipation approach. The development of cracks and failure planes was evaluated using damage properties (D_p) derived from energy dissipation assessment, as calculated using Equation 4. The use of energy dissipation as a reliable indicator of variations in the mechanical properties of the intact specimen has been previously established (Liu et al., 2016; Tan et al., 2019). The damage variable is defined as the ratio of dissipated energy (U_x^d) to constitutive energy (U_x). The constitutive energy was obtained from the stress–strain curve derived from the UCS test, while the dissipated energy is defined as the deviation between constitutive (U_x) and elastic energy (U_x^e). Elastic energy (U_x^e) was calculated based on axial stress (q_x) and the elastic modulus (E_i). Consequently, the damage variable represents the proportion of input energy irreversibly dissipated during deformation, and a higher D_p value indicates a greater degree of internal damage and progressive specimen deterioration during loading.

$$D_p = \frac{U_x^d}{U_x} = \frac{U_x - U_x^e}{U_x} = \frac{U_x - \left(\frac{q_x^2}{2E_i}\right)}{U_x} \tag{4}$$

The D_p value also measures the level of internal damage in a specimen under applied stress. A higher D_p value indicates lower overall strength, as increased damage corresponds to lower ultimate strengths and higher vulnerability to structural failure (Bian et al., 2019; Wang et al., 2021). Moreover, elevated D_p values are associated with a more brittle response, characterized by reduced capacity for plastic deformation. Consequently, such brittleness can lead to sudden failure without clear precursory signs, such as extensive yielding. Conversely, a low D_p value signifies a specimen possessing greater strength, reflecting stronger resistance to damage and a greater capacity to sustain higher loads. These specimens can absorb impact energies while maintaining structural stability with fewer internal defects.

3 RESULTS AND DISCUSSION

3.1 Stress–Strain Behavior and Unconfined Compressive Strength

The stress–strain response of the untreated clay shale reveals its mechanical characteristics, including peak strength, stiffness, and post-failure behavior (Figure 3). Initially, the stress increased linearly with the strain, reaching a maximum stress of about 0.72 MPa. The peak stress occured at a relatively early strain condi-

tion of less than 5%, followed by a residual stress that persisted with 20% strain. On average, the maximum stress (q_u) of the untreated clay shale was 0.72 MPa, at 3.38% strain. The average secant modulus of elasticity (E_{50}) and brittleness index (I_B) were 21.85 MPa and 0.77, respectively. The I_B value indicated that the sample tended to behave brittle rather than ductile. Moreover, intergranular bonds may weaken as the material undergoes stress, contributing to microcracks and fissures within the specimen. This condition resulted in additional friction and resistance, providing additional residual strength. After the failure, microcracks or fractures within the specimen may propagate, forming smaller fragments. These smaller fragments increased the contact surface, creating interlocking effects (Kaiser and Kim, 2015). Statistical analysis of triplicate samples demonstrated good repeatability of the stress–strain response, with coefficients of variation (CoV) for unconfined compressive strength consistently below 12%, indicating that the experimental results are reliable and robust.

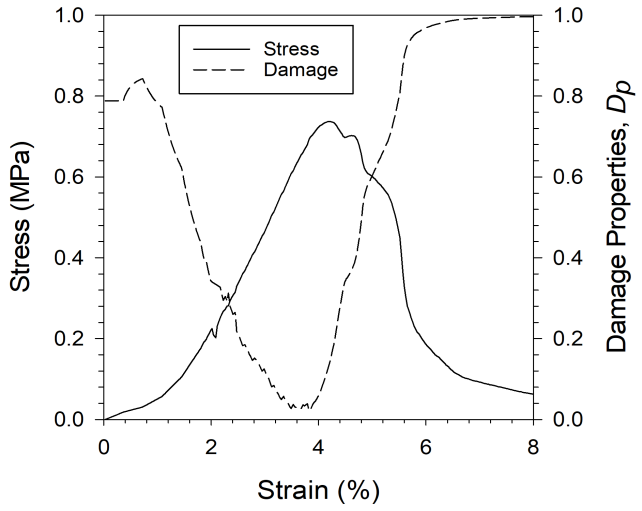

Figure 3. The stress–strain curve of the untreated clay shale.

Geopolymer stabilization modified the stress–strain behavior of clay shale by producing a stronger yet more brittle mechanical response (Figure 4). Each specimen showed no notable difference in behavior within its sample group, indicating consistent mechanical responses. Compared with the untreated condition, the stabilized samples exhibited more brittle behavior (Figure 5 and Figure 6). The increasing brittleness index (I_B) supported this behavior, reflecting the rapid stress drop after specimen failure. All samples displayed a sharp post-failure stress drop with minimal residual stress. This phenomenon stems from soil–geopolymer gel bonding, driven by geopolymerization reactions. Covalent bonds are established between silica and alumina within the geopolymer gel, creating a robust three-dimensional network. As the geopolymer bonds with soil particles, it encapsulates them within the binder matrix, enhancing cohesion and reducing susceptibility to disintegration. This process increases the compressive strength of the stabilized soil. Due to the homogeneous, well–bonded structure, stabilized samples exhibited negligible residual stress upon failure, as the material undergoes more uniform deformation with limited internal particle rearrangement after failure. The increasing I_B (Figure 5) confirms the transition to brittle behavior, with stabilized specimens exhibiting sharp post-failure stress drops and minimal residual stress, consistent with strong geopolymer-soil bonding (Zhang et al., 2020).

The progression of I_B with curing temperature indicates a significant mechanical trade-off (Figure 5). I_B markedly increased with temperature for both activator ratios, indicating a shift toward more brittle failure characteristics. This behavior results from accelerated geopolymerization, which creates a stiff, cemented microstructure that provides high strength but tends to fail in a more catastrophic manner. Mixtures with Ratio B consistently exhibited a higher brittleness index than those with Ratio A, reflecting their role in producing a stiffer and more strongly cemented matrix. Consequently, maximizing strength through high-temperature curing and the use of Ratio B simultaneously increases the brittleness of the stabilized material.

The secant modulus (E_{50}) increases with curing temperature and activator ratio, reflecting the progressive stiffening of the geopolymer–stabilized clay shale. A strong positive correlation was observed between curing temperature and E_{50} for both activator ratios (Figure 6). This trend results from the accelerated geopolymerization reaction kinetics at higher temperatures, which promote the formation of a denser microstructure and a more rigid soil–geopolymer composite. Moreover, mixes with Ratio B consistently exhibited higher E_{50} values across all temperature conditions compared with those with Ratio A. This behavior indicates that the higher silicate concentration in Ratio B facilitates the development of a more robust geopolymer gel structure.

3.2 Effect of Temperature and Alkali Activator Ratio on the Unconfined Compressive Strength

Geopolymer stabilization increases the unconfined compressive strength (q_u) of the clay shale, with strength strongly influenced by curing temperature and activator ratio (Figure 7). The lowest improvement was observed in sample A26, where qu reached 2.70 MPa, equivalent to 3.75 times the strength of the untreated clay shale. The highest strength was obtained when the clay shale was stabilized using an activator with a Na_2SiO_3:NaOH ratio of 2.5 (Ratio B) and cured at 60°C (sample B60), producing an average qu of 11.49 MPa,

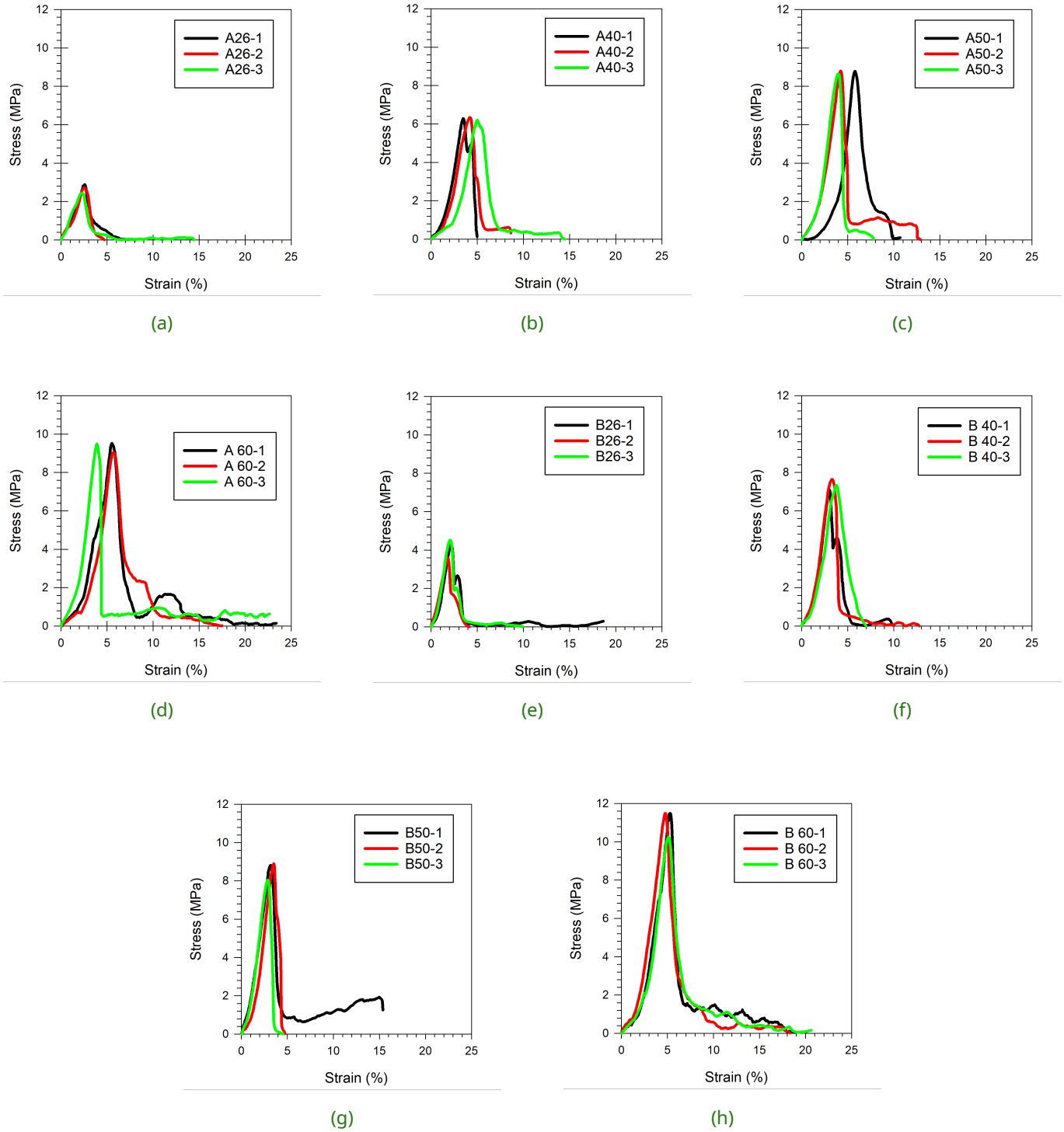

Figure 4. The stress-strain curve of sample (a) A26, (b) A40, (c) A50, (d) A60, (e) B26, (f) B40, (g) B50, and (h) B60.

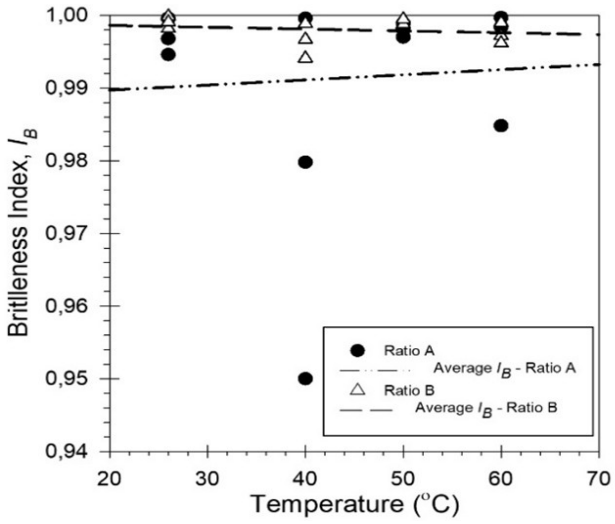

Figure 5. The average of the Brittleness Index.

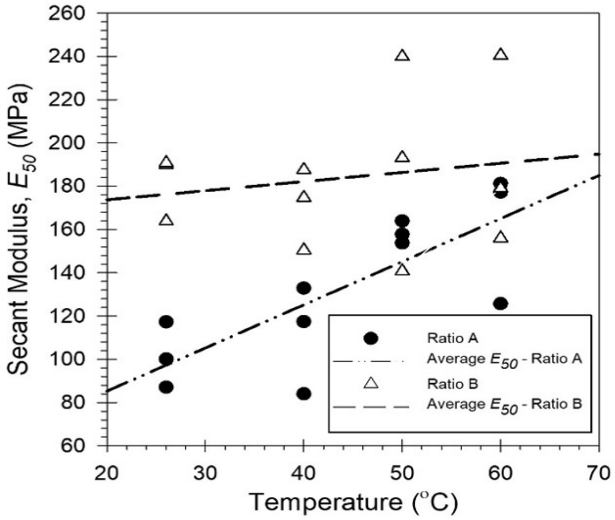

Figure 6. The Secant Modulus.

or 15.95 times that of the untreated sample. Although samples prepared with Ratio A and Ratio B generally exhibited similar trends with increasing curing temperature, Ratio B consistently yielded higher strength values. At a 50°C curing temperature, the difference in UCS between Ratios A and B was relatively small, whereas at other temperatures, Ratio B performed better. The average peak stress for samples A26, A40, A50, and A60 was 2.67 MPa, 6.32 MPa, 8.79 MPa, and 9.28 MPa, respectively. In comparison, specimens B26, B40, B50, and B60 reached average peak stresses of 3.94 MPa, 7.37 MPa, 8.86 MPa, and 11.49 MPa, respectively.

The effectiveness of geopolymer stabilization depends not only on curing temperature but also on the availability of reactive alumina and silica supplied by the activator system. The present results demonstrate that geopolymer treatment enhanced the unconfined compressive strength of the clay shale, while elevated curing temperature accelerated the geopolymerization reaction. However, if the required quantities of alumina and silica are insufficient, the resulting strength improvement may not reach its optimum potential. The activator plays a crucial role in dissolving alumina and silica from fly ash (precursor). In activators with Ratio A, the amount of soluble aluminosilicate may be insufficient to sustain the increasingly rapid reaction rate at higher curing temperatures. To address this limitation, adjustments can be made not only to the quantity but also to the composition ratio of the activator. Samples with Ratio B exhibited superior performance when cured at room temperature (26°C) and elevated temperature (60°C), which can be attributed to the addition of soluble silicate Na_2SiO_3 in the activator. The higher amount of silica enhances the effectiveness of Si–O–Si bonds, which tend to be stronger than Si–O–Al and Al–O–Al bonds (Kaiser and Kim, 2015).

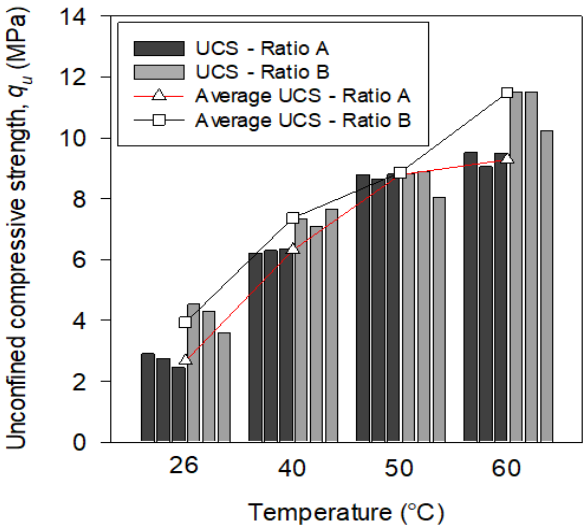

Figure 7. The UCS from each test of samples with different alkali activator ratio and curing.

3.3 The Damage Properties

Damage analysis provides micromechanical insight into the failure behavior of geopolymer-stabilized specimens by linking energy dissipation with the observed stress–strain response (Figure 8). The solid line represents the stress–strain curve obtained from the UCS test, while the dashed line represents the damage–strain curve calculated using Equation (4). The damage property (D_p) effectively quantifies the samples' gradual energy dissipation and internal degradation. Higher curing temperatures shift the failure point toward greater dissipated energy at larger strain values. Test results also indicated the development of a wider elastic zone during initial loading stage at elevated temperatures, suggesting a more extended process of pore and crack compaction. However, higher curing

temperatures may also promote excessive pore formation, likely caused by accelerated water evaporation during curing, which can increase material porosity (Duxson and Provis, 2008; Odeh and Al-Rkaby, 2022; Provis, 2018). This issue could be mitigated by extending the curing duration, allowing more time for geopolymer gel formation and enabling the gel to fill existing pores within the soil matrix.

The evolution of the damage property (D_p) further clarifies the influence of curing temperature and activator composition on the failure behavior of the stabilized specimens. The samples cured at 60°C swiftly reached a damage state of D_p=1 at low strains, corroborating their brittle characteristics as indicated by a high I_B. Conversely, samples cured at ambient temperature exhibited a more progressive increase in D_p, signifying an enhanced ability for plastic deformation and energy absorption before total failure. Moreover, the more pronounced post-peak D_p gradient in Ratio B samples relative to Ratio A at comparable temperatures offered a damage-oriented rationale for its elevated brittleness index. These findings indicate that intensified geopolymerization driven by elevated temperature and alkali concentration produces a dense and strong microstructure that, while mechanically robust, is more susceptible to rapid and catastrophic damage propagation.

Activator composition plays a critical role in controlling the ductility and failure characteristics of geopolymer–stabilized clay shale. Specimens prepared with Ratio A failed at higher strains than those prepared with Ratio B, indicating a more ductile response. This behavior likely reflects the formation of a less rigid geopolymer matrix, which permitted greater plastic deformation and may be beneficial for applications requiring energy absorption and resilience. By contrast, specimens prepared with Ratio B developed a denser and stiffer geopolymer framework, resulting in higher strength but lower ductility. Their failure at lower strains therefore indicates a more brittle mechanical response. This stiffer matrix may be associated with enhanced formation of sodium aluminosilicate hydrate (N–A–S–H) gel, which improves microstructural continuity and promotes polymerization when the sodium silicate content is increased (Lv et al., 2021). In addition, increased curing temperatures can reduce pore volume and promote the formation of an amorphous porous network due to accelerated geopolymerization (Wang et al., 2013). The modulus of sodium silicate also significantly influences the density and porosity of the geopolymer structure, where an optimal modulus promotes more complete alkali activation and the formation of a denser matrix (Adhikari et al., 2020; Gao et al., 2021; Morsy et al., 2014). Further investigation into the Si/Al and Na/Al molar ratios could provide deeper insights into the microstructural evolution and macroscopic mechanical properties of the geopolymer, as these ratios significantly impact the polymerization efficiency and network density (Wang et al., 2021).

The test result showed that all treated soils' unconfined compressive strength (q_u) increased significantly depending on the curing temperature. Samples cured at 26°C (room ambient) exhibited increases of approximately 3.45 times (Ratio A) and 2.78 times (Ratio B) when the curing temperature was raised from 26°C to 60°C. Such dependence of peak qu on curing temperature can be attributed to a faster chemical reaction between the aluminosilicate materials and activators at a higher temperature. Hence, the reaction leads to a more rapid formation of geopolymer bonds. This accelerated reaction contributes to the early strength development of geopolymers (Aredes et al., 2015).

Increasing the alkali activator ratio further influences strength development, although its effectiveness depends on curing temperature and reaction kinetics. Raising the Na_2SiO_3:NaOH ratio to 2.5 resulted in qu increases of 1.54, 1.17, 1.01, and 1.23 times compared with samples prepared with a ratio of 2.0 at curing temperatures of 26°C, 40°C, 50°C, and 60°C, respectively. However, the effectiveness of increasing the amount of Na_2SiO_3 in the activator did not show a consistent result. At 50°C, for instance, no significant strength improvement was observed. This condition may indicate silica deficiency under highly accelerated reaction kinetics at elevated temperatures. As a result, a less stable, alumina–rich geopolymer gel forms and potentially entraps unreacted fly ash particles, limiting further strength development (Sarkar and Routray, 2018). Previous studies stated that the aluminosilicate gel formation depends on the soluble silica concentration in the activator and the alkalinity (amount of NaOH), which affects the degree of polymerization (Abdullah et al., 2020). In this process, hydroxide ions (OH^-) catalyze the dissolution of aluminosilicate species, while the alkaline metal cations contribute to structural formation by balancing the negative charge of tetrahedral aluminum within the geopolymer framework (Duxson et al., 2007).

Sensitivity analysis showed that temperature had a more substantial impact on the UCS than the alkali activator ratio, where a 10°C temperature increase led to an average 40–60% strength gain, whereas increasing the alkali activator ratio from 2.0 to 2.5 caused a 15–20% rise. Although this study was conducted using clay shale from Indonesia, the results are relevant to regions experiencing high ambient temperatures, such as the Middle East, South Asia, and other arid zones where ground temperatures may approach 50°C. The ability of fly ash–based geopolymer stabilization to maintain and even enhance strength under elevated curing temperatures up to 60°C suggests its potential as a scalable solution for stabilizing clay–rich soils in climates subject to thermal extremes. While the re-

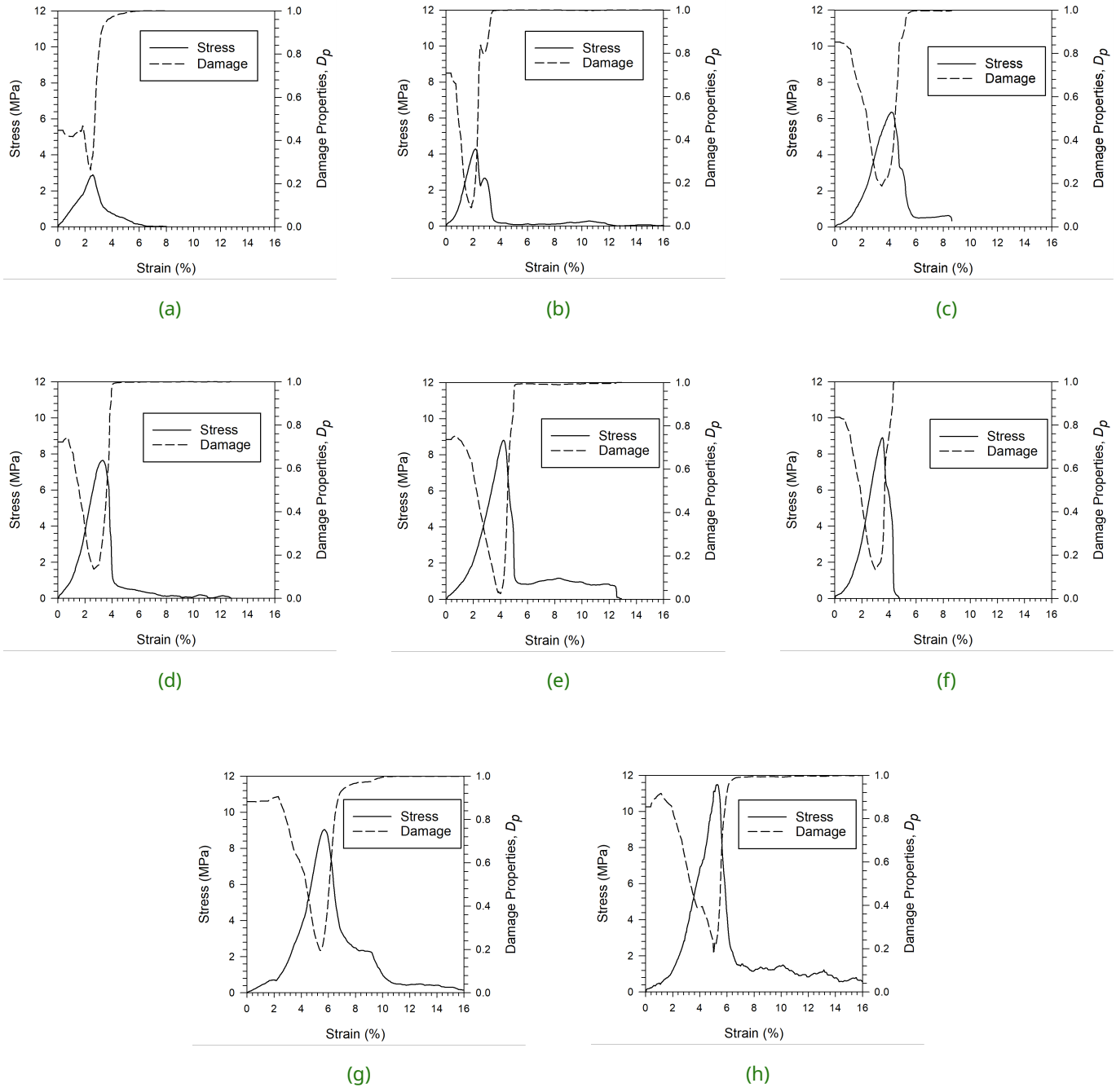

Figure 8. Damage Properties of sample (a) A26-1, (b) B26-1, (c) A40-1, (d) B40-1, (e) A50-1, (f) B50-1, (g) A60-1, and (h) B60-1.

sults are based on a 7–day curing period in a controlled laboratory setting, they provide important insight into the temperature-dependent behaviour of geopolymer–stabilized clay shale. This curing duration represents a meaningful indicator of short–term strength development, which is particularly relevant for projects requiring rapid soil stabilization. Nevertheless, it does not adequately reflect the enduring strength and resilience necessary for permanent infrastructure. The 7–day results may underestimate the final strength due to the continued geopolymerization process. Consequently, subsequent research should concentrate on long-term efficacy (28–90 days), resilience against environmental fluctuations, and verification via field trials to ascertain this sustainable stabilization technique's practical feasibility and scalability.

4 CONCLUSION

This study investigated the unconfined compressive strength (UCS, q_u) and damage properties (D_p) of clay shale stabilized with fly ash–based geopolymer under different curing temperatures and alkali activator ratios. The results demonstrated that elevated curing temperature increased the unconfined compressive strength of the stabilized soil by accelerating the geopolymerization reaction between fly ash and the alkali activator and promoting the formation of sodium aluminosilicate hydrate gel. Nevertheless, activator composition also had a pronounced influence on strength development. Specimens prepared with Ratio B (Na_2SiO_3:NaOH = 2.5) showed greater strength enhancement due to the higher silica availability provided by Na_2SiO_3. In contrast, specimens prepared with Ratio A (Na_2SiO_3:NaOH = 2.0) exhibited a stagnation in strength development at curing temperatures of 50°C and above. This trend may be attributed to an imbalance in geopolymerization under silica–deficient conditions at highly accelerated reaction rates, leading to the formation of a less stable alumina–rich geopolymer gel and the entrapment of unreacted fly ash particles, which ultimately limited further strength gain.

All test results consistently showed an expanding elastic zone at the initial loading stage as curing temperature increases. This behavior is attributed to the higher initial stiffness of the sodium–aluminosilicate–hydrate gel structure. In addition, specimens treated with Ratio A reached failure at higher strain levels than those treated with Ratio B, indicating a more ductile mechanical response. This difference likely results from the less rigid geopolymer matrix formed with Ratio A, which allows greater plastic deformation. These findings contribute to the advancement of sustainable soil stabilization by providing new insights into the temperature-dependent behavior of geopolymer–stabilized clay shale. Nevertheless, this study has several limitations, including controlled laboratory conditions and a relatively short curing period, which may not fully represent field conditions. Future research should focus on long–term durability under environmental exposure, field–scale implementation, microstructural characterization, and the development of low–alkali activators to improve the sustainability and cost–effectiveness of this stabilization method. By enhancing the understanding of geopolymer–soil interactions, this study supports the adoption of environmentally friendly alternatives to conventional cement-based stabilization in geotechnical engineering.

DISCLAIMER

The authors declare no conflict of interest.

ACKNOWLEDGMENTS

The authors are grateful to the Directorate of Research, Technology, and Community Service of the Ministry of Education, Culture, Research and Technology of the Republic of Indonesia for Research Funding under the Fundamental Research scheme with contract number 0609.7/LL5INT/AL.04/2024, and the Research and Innovation Center of Universitas Muhammadiyah Yogyakarta for assistance during the research.

REFERENCES

Abdullah, H. H., Shahin, M. A., Walske, M. L. and Karrech, A. (2020), 'Systematic approach to assessing the applicability of fly-ash-based geopolymer for clay stabilization', *Canadian Geotechnical Journal* **57**, 1356–1368.
URL: *https://doi.org/10.1139/cgj-2019-0215*

Abdullah, M., Ahmad, F. and Mustafa Al Bakri, A. (2015), 'Geopolymer application in soil: A short review', *Applied Mechanics and Materials* **754**, 378–381.
URL: *https://doi.org/10.4028/www.scientific.net/AMM.754-755.378*

Abdullah, M. M. A. B., Kamarudin, H., Bnhussain, M., Ismail, K. N., Rafiza, A. and Zarina, Y. (2011), 'The relationship of naoh molarity, na2sio3/naoh ratio, fly ash/alkaline activator ratio, and curing temperature to the strength of fly ash-based geopolymer', *Advanced Materials Research* **328**, 1475–1482.
URL: *https://doi.org/10.4028/www.scientific.net/AMR.328-330.1475*

Abdullah, M. S. and Ahmad, F. (2017), Effect of alkaline activator to fly ash ratio for geopolymer stabilized soil, *in* 'MATEC Web of Conferences', EDP Sciences, p. 01012.
URL: *https://doi.org/10.1051/matecconf/20179701012*

Adhikari, S., Khattak, M. J. and Adhikari, B. (2020), 'Mechanical characteristics of soil-rap-geopolymer mixtures for road base and subbase layers', *International Journal of Pavement Engineering* **21**(4), 483–496.
URL: *https://doi.org/10.1080/10298436.2018.149213*

Aredes, F., Campos, T., Machado, J., Sakane, K., Thim, G. and Brunelli, D. (2015), 'Effect of cure temperature on the formation of metakaolinite-based geopolymer', *Ceramics International* **41**, 7302–7311.
URL: *https://doi.org/10.1016/j.ceramint.2015.02.022*

Ayub, F. and Khan, S. A. (2023), 'An overview of geopolymer composites for stabilization of soft soils', *Construction and Building Materials* **404**, 133195.
URL: *https://doi.org/10.1016/j.conbuildmat.2023.133195*

Bian, K., Liu, J., Zhang, W., Zheng, X., Ni, S. and Liu, Z. (2019), 'Mechanical behavior and damage constitutive model of rock subjected to water-weakening effect and uniaxial loading', *Rock Mechanics and Rock Engineering* **52**, 97–106.
URL: *https://doi.org/10.1007/s00603-018-1580-4*

Diana, W., Hartono, E. and Damayanti, I. (2025), The durability of clay-fly ash-based geopolymer: The variation on curing temperature, *in* 'AIP Conference Proceedings'.
URL: *https://doi.org/10.1063/5.0280478*

Diana, W., Hartono, E. and Kusuma, A. W. (2025), Optimizing strength in marine sand-fly ash geopolymers: The impact of alkali activator ratios and curing temperatures, *in* 'Lecture Notes in Civil Engineering', pp. 165–173.
URL: *https://doi.org/10.1007/978-981-96-2143-9_18*

Diana, W., Ma'rifah, R. and Hartono, E. (2025), The tensile strength of marine sand using fly ash-based geopolymer: Influence of sodium hydroxide concentration and alkaline activator ratio, *in* 'Journal of Physics: Conference Series', IOP Publishing, p. 012038.
URL: *https://doi.org/10.1088/1742-6596/2989/1/012038*

Duxson, P., Fernández-Jiménez, A., Provis, J. L., Lukey, G. C., Palomo, A. and Van Deventer, J. S. (2007), 'Geopolymer technology: The current state of the art', *Journal of Materials Science* **42**, 2917–2933.
URL: *https://doi.org/10.1007/s10853-006-0637-z*

Duxson, P. and Provis, J. L. (2008), 'Designing precursors for geopolymer cements', *Journal of the American Ceramic Society* **91**, 3864–3869.
URL: *https://doi.org/10.1111/j.1551-2916.2008.02787.x*

Gao, Y., Feng, Y., Tong, G. and Tang, X. (2021), Influences of sodium silicate modulus on mechanical properties and microstructure of fly ash geopolymer, *in* 'IOP Conference Series: Earth and Environmental Science', p. 012056.
URL: *https://doi.org/10.1088/1755-1315/760/1/012056*

Ghadir, P. and Ranjbar, N. (2018), 'Clayey soil stabilization using geopolymer and portland cement', *Construction and Building Materials* **188**, 361–371.
URL: *https://doi.org/10.1016/j.conbuildmat.2018.07.207*

Hartono, E., Diana, W. and Bahti, F. N. (2023), Unconfined compressive strength test on geopolymer fly ash stabilized clay shale, *in* 'E3S Web of Conferences', Vol. 429, pp. 1–6.
URL: *https://doi.org/10.1051/e3sconf/202342904025*

Hartono, E., Diana, W. and Hendriana, J. W. (2023), Study of compressive strength and durability of geopolymer stabilized clay shale with fly ash binder and 12m naoh content, *in* 'AIP Conference Proceedings'.
URL: *https://doi.org/10.1063/5.0154887*

Hartono, E., Muntohar, A. and Abiyoga, N. (2021), Influence of the pulverised method on the plasticity and strength behaviour of cement stabilised clayshale and sandstone, *in* 'IOP Conference Series: Materials Science and Engineering', IOP Publishing, p. 012096.
URL: *https://doi.org/10.1088/1757-899X/1144/1/012096*

Kaiser, P. K. and Kim, B.-H. (2015), 'Characterization of strength of intact brittle rock considering confinement-dependent failure processes', *Rock Mechanics and Rock Engineering* **48**, 107–119.
URL: *https://doi.org/10.1007/s00603-014-0545-5*

Khanday, S. A., Hussain, M. and Das, A. K. (2021), 'Rice husk ash-based geopolymer stabilization of indian peat: Experimental investigation', *Journal of Materials in Civil Engineering* **33**(12), 04021347.
URL: *https://doi.org/10.1061/(ASCE)MT.1943-5533.000398*

Khasib, I. A., Daud, N. N. N. and Nasir, N. A. M. (2021), 'Strength development and microstructural behavior of soils stabilized with palm oil fuel ash (pofa)-based geopolymer', *Applied Sciences* **11**(8), 3572.
URL: *https://doi.org/10.3390/app11083572*

Liu, X., Ning, J., Tan, Y. and Gu, Q. (2016), 'Damage constitutive model based on energy dissipation for intact rock subjected to cyclic loading', *International Journal of Rock Mechanics and Mining Sciences* **85**, 27–32.
URL: *https://doi.org/10.1016/j.ijrmms.2016.03.003*

Luo, Z. and Zhang, B. (2023), 'Effect of humic acid and fulvic acid on mechanical and durability properties of geopolymer stabilized soft soil', *Construction and Building Materials* **409**, 133875.
URL: *https://doi.org/10.1016/j.conbuildmat.2023.133875*

Lv, Q., Yu, J., Ji, F., Gu, L., Chen, Y. and Shan, X. (2021), 'Mechanical property and microstructure of fly ash-based geopolymer activated by sodium silicate', *KSCE Journal of Civil Engineering* **25**(5), 1765–1777.
URL: *https://doi.org/10.1007/s12205-021-0025-x*

Miraki, H., Shariatmadari, N., Ghadir, P., Jahandari, S., Tao, Z. and Siddique, R. (2022), 'Clayey soil stabilization using alkali-activated volcanic ash and slag', *Journal of Rock Mechanics and Geotechnical Engineering* **14**, 576–591.
URL: *https://doi.org/10.1016/j.jrmge.2021.08.012*

Morsy, M. S., Alsayed, S. H., Al-Salloum, Y. and Almusallam, T. (2014), 'Effect of sodium silicate to sodium hydroxide ratios on strength and microstructure of fly ash geopolymer binder', *Arabian Journal for Science and Engineering* **39**(6), 4333–4339.
URL: *https://doi.org/10.1007/s13369-014-1093-8*

Odeh, N. A. and Al-Rkaby, A. H. (2022), 'Strength, durability, and microstructures characterization of sustainable geopolymer improved clayey soil', *Case Studies in Construction Materials* **16**, e00988.
URL: *https://doi.org/10.1016/j.cscm.2022.e00988*

Phetchuay, C., Horpibulsuk, S., Arulrajah, A., Suksiripattanapong, C. and Udomchai, A. (2016), 'Strength development in soft marine clay stabilized by fly ash and calcium carbide residue based geopolymer', *Applied Clay Science* **127**, 134–142.
URL: *https://www.sciencedirect.com/science/article/pii/S0169131716301570*

Provis, J. L. (2018), 'Alkali-activated materials', *Cement and Concrete Research* **114**, 40–48.
URL: *https://doi.org/10.1016/j.cemconres.2017.02.009*

Razeghi, H. R., Geranghadr, A., Safaee, F., Ghadir, P. and Javadi, A. A. (2024), 'Effect of co2 exposure on the mechanical strength of geopolymer-stabilized sandy soils', *Journal of Rock Mechanics and Geotechnical Engineering* **16**(2), 670–681.
URL: *https://doi.org/https://doi.org/10.1016/j.jrmge.2023.04.017*

Rivera, J. F., Orobio, A., Cristelo, N. and De Gutierrez, R. M. (2020), 'Fly ash-based geopolymer as a4 type soil stabiliser', *Transportation Geotechnics* **25**, 100409.
URL: *https://doi.org/10.1016/j.trgeo.2020.100409*

Sarkar, R. and Routray, S. P. (2018), 'Fly ash containing alkali activated geopolymer concrete: Effect of the na2sio3:naoh ratio and temperature', *Interceram-International Ceramic Review* **67**(3), 24–29.
URL: *https://doi.org/10.1007/s42411-018-0014-3*

Simatupang, P. T., Alatas, I. M., Redyananda, A. K. and Purnomo, E. A. (2022), 'Shear strength and durability behaviors of compacted weathered clay shale mixture using portland cement', *Journal of the Civil Engineering Forum* **8**(2), 169–178.
URL: *https://doi.org/10.22146/jcef.3491*

Tan, Y., Gu, Q., Ning, J., Liu, X., Jia, Z. and Huang, D. (2019), 'Uniaxial compression behavior of cement mortar and its damage-constitutive model based on energy theory', *Materials* **12**, 1309.
URL: *https://doi.org/10.3390/ma12081309*

Van Deventer, J., Provis, J., Duxson, P. and Lukey, G. (2007), 'Reaction mechanisms in the geopolymeric conversion of inorganic waste to useful products', *Journal of Hazardous Materials* **139**, 506–513.
URL: *https://doi.org/10.1016/j.jhazmat.2006.02.044*

Wang, J., Fu, J., Song, W. and Zhang, Y. (2021), 'Mechanical properties, damage evolution, and constitutive model of rock-encased backfill under uniaxial compression', *Construction and Building Materials* **285**, 122898.
URL: *https://doi.org/10.1016/j.conbuildmat.2021.122898*

Wang, Y. C., Zhang, Y. J., Xu, D. L. and Liu, L. C. (2013), 'Influence of different curing temperatures on mechanical properties of alkali activated silica fume and fly ash based geopolymer', *Materials Research Innovations* **17**(sup1), 21–25.
URL: *https://doi.org/10.1179/1432891713Z.000000000191*

Wong, B. Y. F., Wong, K. S. and Phang, I. R. K. (2019), A review on geopolymerisation in soil stabilization, *in* 'IOP Conference Series: Materials Science and Engineering', p. 012070.
URL: *https://doi.org/10.1088/1757-899X/495/1/012070*

Xu, H. and Van Deventer, J. S. (2002), 'Geopolymerisation of multiple minerals', *Minerals Engineering* **15**(12), 1131–1139.
URL: *https://doi.org/10.1016/S0892-6875(02)00255-8*

Zhang, H., Li, L., Yuan, C., Wang, Q., Sarker, P. K. and Shi, X. (2020), 'Deterioration of ambient-cured and heat-cured fly ash geopolymer concrete by high temperature exposure and prediction of its residual compressive strength', *Construction and Building Materials* **262**, 120924.
URL: *https://doi.org/10.1016/j.conbuildmat.2020.120924*

Zhang, M., Guo, H., El-Korchi, T., Zhang, G. and Tao, M. (2013), 'Experimental feasibility study of geopolymer as the next-generation soil stabilizer', *Construction and Building Materials* **47**, 1468–1478.
URL: *https://doi.org/10.1016/j.conbuildmat.2013.06.017*